



Minimising soil organic carbon erosion by wind is critical for land degradation neutrality

Adrian Chappell^{a,*}, Nicholas P. Webb^b, John F. Leys^c, Cathleen M. Waters^d, Susan Orgill^e, Michael J. Eyres^f

^a School of Earth and Ocean Sciences, Cardiff University, Wales, CF10 3AT, UK

^b USDA-ARS Jornada Experimental Range, Las Cruces, NM, USA

^c Knowledge Services Team, Science Division, NSW Environment and Heritage, Gunnedah, NSW 2380, Australia

^d NSW Department of Primary Industries, PMB 19, Trangie, NSW, 2823, Australia

^e NSW Department of Primary Industries, Pine Gully Road, Wagga Wagga, NSW, 2650, Australia

^f Field Systems (Australia), Stirling, SA, 5152, Australia



ARTICLE INFO

Keywords:

Land degradation neutrality
Soil organic carbon
Land cover
Wind erosion
Sequestration

ABSTRACT

The Land Degradation-Neutrality (LDN) framework of the United Nations Convention to Combat Desertification (UNCCD) is underpinned by three complementary interactive indicators (metrics: vegetation cover, net primary productivity; NPP and soil organic carbon; SOC) as proxies for change in land-based natural capital. The LDN framework assumes that SOC changes slowly, primarily by decomposition and respiration of CO₂ to the atmosphere. However, there is growing evidence that soil erosion by wind, water and tillage also reduces SOC stocks rapidly after land use and cover change. Here, we modify a physically-based wind erosion sediment transport model to better represent the vegetation cover (using land surface aerodynamic roughness; that is the plant canopy coverage, stone cover, soil aggregates, etc. that protects the soil surface from wind erosion) and quantify the contribution of wind erosion to global SOC erosion (2001–2016). We use the wind erosion model to identify global dryland regions where SOC erosion by wind may be a significant problem for achieving LDN. Selected sites in global drylands also show SOC erosion by wind accelerating over time. Without targeting and reducing SOC erosion, management practices in these regions will fail to sequester SOC and reduce land degradation. We describe the interrelated nature of the LDN indicators, the importance of including SOC erosion by wind erosion and how by explicitly accounting for wind erosion processes, we can better represent the physical effects of changing land cover on land degradation. Our results for Earth's drylands show that modelling SOC stock reduction by wind erosion is better than using land cover and SOC independently. Furthermore, emphasising the role of wind erosion in UNCCD and Intergovernmental Panel on Climate Change (IPCC) reporting will better support LDN and climate change mitigation and adaptation globally.

1. Introduction

Humans have substantially impacted the Earth's surface via land cover change (LCC) associated with widespread land use change (LUC) and an intensification of land management practices (Luysaert et al., 2014). Early agriculture exploited the soil's natural balance of inputs and losses of nutrients and soil organic carbon (SOC) to feed a rapidly expanding global population (Amundson et al., 2015; Fig. 1). However, in many regions agriculture has accelerated the loss of fertile topsoil by wind, water and tillage erosion to orders of magnitude greater than soil formation (Amundson et al., 2015; Fig. 1). This reduces soil nutrient capacity and soil profile water content, thus representing a major threat

to the productive potential of landscapes (FAO and ITPS, 2015). Accelerated soil erosion changes every biophysical and biogeochemical cycle, perturbing the cycles of C, dust, energy and water and degrades soil and air quality which impact global socio-economic systems. Soil erosion therefore represents one of the most important and highly synergistic processes of land degradation. For example, the loss of soil by wind erosion reduces the depth of soil and its potential to support agricultural production (Webb et al., 2017). Wind erosion also causes dust emission and the preferential removal of fine, C- and nutrient-rich material (Chappell et al., 2013). Vegetation species change in response to the redistribution and loss of soil nutrients and possible change in soil hydrology. Typically, as vegetation cover declines, the sheltering of

* Corresponding author.

E-mail address: chappella2@cardiff.ac.uk (A. Chappell).

<https://doi.org/10.1016/j.envsci.2018.12.020>

Received 19 May 2018; Received in revised form 29 November 2018; Accepted 14 December 2018

Available online 21 December 2018

1462-9011/ Crown Copyright © 2018 Published by Elsevier Ltd. All rights reserved.

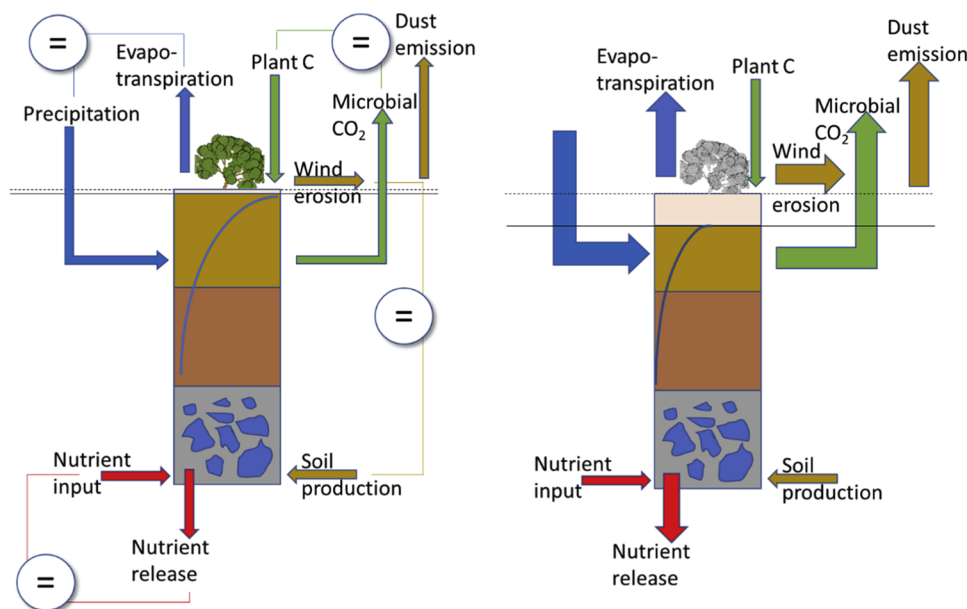


Fig. 1. Steady states (=) in Earth's systems are perturbed by human activity causing accelerated soil erosion which feedback and interact (synergistic) to changes in the biophysical and biogeochemical cycles, altering system balance. (adapted from Amundson et al., 2015).

bare surfaces is reduced causing wind erosion to accelerate. Such feedbacks can be a key driver of regional ecosystem change (Bestelmeyer et al., 2015).

Wind and water erosion influence the flux and stock of SOC lost from soil in several ways. There is considerable debate about the fate of SOC removed by soil erosion with some studies suggesting it may be dynamically replaced (Stallard, 1998), protected after deposition (Van Oost et al., 2007) thereby representing a potential C sink (Dialynas et al., 2016), or more exposed to mineralisation during erosion and transport (Lal, 2004, 2005) which may change the prevailing chemistry of the eroded OM (Ellerbrock et al., 2016; Sommer et al., 2016). Organic matter is preferentially removed from soil during erosion due to its low density and this primarily occurs at the soil surface (with the exception of gully and rill erosion) where the concentration of OC is greatest (Gregorich et al., 1998; Lal, 2003). Consequently, eroded sediment is estimated to be up to five times more enriched with OC than most topsoil (Lal, 2003). Organic matter in eroded sediment is then more vulnerable to mineralisation through direct exposure and oxidation, or through the degradation of aggregates where OM is occluded (Lal, 2003, 2005; Nguyen et al., 2008). Wind erosion degrades macroaggregates thereby accelerating OM mineralisation (Elliott, 1986; Li et al., 2014; Singh and Singh, 1996). Furthermore, large dust emission events may transport fine eroded sediment (e.g., less than 22 μm) offshore (Leys et al., 2011) thereby representing a loss of C from the terrestrial system (Chappell et al., 2013).

About 11% of the Earth's land surface is agricultural land, of which 80% suffers moderate erosion (Pimentel, 1993). Since farming began, an area greater than the Earth's cropland has been abandoned due to erosion (Lal, 1990). The total economic value of erosion-induced loss is estimated at USD400 billion per year from arable land alone (FAO and ITPS, 2015) and some 10 million ha of cropland worldwide is abandoned each year due to soil erosion (Faeth and Crosson, 1994). The World Health Organisation (WHO) reported more than 3.7 billion people worldwide are malnourished (WHO, 2004). The vast majority of affected developing countries are in drylands where soil erosion is greatest. If accelerated erosion continues unabated, yield reduction by 2020 may be 14.5% for sub-Saharan Africa (Lal, 1995). Climate projections of greater rainfall intensity, reduced soil moisture and increased wind gustiness may cause increases in both wind and water

erosion. Increased competition for land is expected to increase social and political instability, exacerbate food insecurity, poverty, conflict, and migration (UN-Habitat-GLTN, 2016)

To address the threat of land degradation to agriculture, ecosystems and society, in 2015 the United Nations Convention to Combat Desertification (UNCCD) endorsed Sustainable Development Goal (SDG) target 15.3 – Land Degradation-Neutrality (LDN), defined as “a state whereby the amount and quality of land resources necessary to support ecosystem functions and services and enhance food security remain stable or increase within specified temporal and spatial scales and ecosystems” (UNCCD, 2015). The concept aims to maintain and / or renew the global resource of healthy and productive land by avoiding, reducing, or reversing land degradation. The complex interplay between drivers / pressures, degradation processes, the flows for ecosystem services and human needs and indicators of change are established in the framework (Cowie et al., 2018 see Fig. 3).

Three indicators were selected by the UNCCD to evaluate LDN through change in the land-based natural capital: land cover (metric: physical land cover), land productivity (metric: net primary productivity; NPP) and carbon stocks (metric: soil organic carbon; SOC). Change in vegetative cover was assumed highly responsive to land use dynamics e.g., land conversion. Land productivity was selected to represent relatively fast changes in ecosystem function. Carbon stocks were assumed to represent “...slower changes resulting from the net effects of biomass growth and disturbance/removal...” and to be used as an indicator of agroecosystem resilience (Cowie et al., 2018; p. 32). In short, the indicators and associated metrics of ecosystems services are used to monitor neutrality relative to a baseline and by comparison with gains and losses.

The interrelated nature of the LDN indicators, and the role of SOC erosion, can be illustrated with a reduced complexity framework for estimating change in SOC stocks in Earth System Models and interpreting measured SOC change (Todd-Brown et al., 2013). The framework assumes that the soil organic carbon (C) pool in area i is at steady state such that NPP (kg C m^{-2}) inputs equal outputs from heterotrophic respiration (R ; kg C m^{-2})

$$0 = \frac{dC_i}{dt} = NPP_i - R_i. \quad (1)$$

Similarly, it assumes that R_i is directly proportional to C_i with a

spatially uniform decomposition rate constant k (Parton et al., 1987).

$$R_i = kC_i. \quad (2)$$

Combining the two above equations produces a model in which C_i is proportional to NPP and inversely proportional to a global decomposition rate (k)

$$C_i = \frac{NPP_i}{k}. \quad (3)$$

Consistent with Chappell et al. (2015) and others (e.g., Doetterl et al., 2012; Regnier et al., 2013), C_i is also controlled by wind and water erosion (E_a ; $\text{g soil m}^{-2} \text{s}^{-1}$) and land cover is one of the main controls on erosion. Land cover is used in the LDN as a surrogate for erosion. Considering the erosion process, and not just the indicator land cover, and explicitly accounting for the effects of erosion on SOC stocks, are important because land cover alone and C budgets used to assess stocks typically do not quantify the erosion impact on the soil resource (specifically C_i). At best, land cover indicates only that the resource is at risk. By making specific use of land cover to represent E_a , the framework can be completed:

$$C_i = \frac{NPP_i - E_a}{k}. \quad (4)$$

The framework demonstrates the interrelated, overlapping nature of the LDN indicators and the critical role played by E_a . Here, our objective is to show that in global drylands, SOC stocks are reduced rapidly after land use / land management induced land cover change by wind erosion. We have restricted our estimates of soil erosion to wind (E) for simplicity and use recent developments of a physically-based sediment transport model to enable consistent global estimation of wind erosion in response to land cover change (Chappell and Webb, 2016). We show that E provides essential and valuable information about the changing condition of the soil resource and should be considered formally in assessing C stocks as the basis for evaluating LDN.

2. Methods and data

2.1. Wind erosion model

Physical land cover is a key indicator of land use, land cover and land management change. Land cover is also one of the main factors controlling wind erosion and is most easily managed to protect the soil from erosive forces of the wind. However, land cover itself is not sufficient to explain the occurrence of wind erosion and related vegetation indices provide only crude approximations for wind erosion assessment (Chappell et al., 2017). Vegetation structure, density and distribution (width, breadth, height and spacing) plays a critical role in the protection of the soil from wind erosion and subsequent dust emission. Vegetation extracts momentum from the wind and shelters downstream areas (behind or in the lee or wake of the vegetation) in proportion to wind speed (Fig. 2).

Chappell and Webb (2016) developed a new approach to wind erosion modelling which established a relation between sheltered area and the proportion of shadow over a given area; the inverse of direct beam directional (at-nadir) hemispherical reflectance (black sky albedo; BSA; Chappell et al., 2010). Once normalised by the surface reflectance and rescaled, ω_{ns} provides the proportion of shadow and has

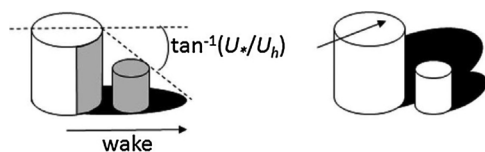


Fig. 2. The (a) Raupach (1992) concept for reducing the complexity of aerodynamic roughness and its representation (b) using shadow by Chappell et al. (2010) to enable an approximation from satellite remote sensing.

been calibrated against wind tunnel measurements of several key aerodynamic properties that control wind erosion. For example, Chappell and Webb (2016) established a strong relation between ω_{ns} and the wind shear stress at the soil surface (u_{*s} ; m s^{-1}) scaled by freestream wind speed (U_f ; m s^{-1} ; Fig. 2). These variables drive aeolian sediment transport (Q_h ; $\text{g m}^{-1} \text{s}^{-1}$) for a given size fraction d :

$$Q_h(d) = c \frac{\rho}{g} u_{*s}^3 \left(1 - \left(\frac{u_{*ts}(d)H(w)}{u_{*s}} \right) \right), \quad (5)$$

where c is a fitting parameter used to adjust the magnitude of the model output, ρ is the density of air (1.23 kg m^{-3}), g is acceleration due to gravity (9.81 m s^{-2}), u_{*ts} is the soil threshold shear stress of a bare, smooth (no roughness elements) below which sediment transport does not occur (Shao et al., 1996) and $H(w)$ is a function of soil moisture which also inhibits transport (Fecan et al., 1999). The model therefore adjusts the total available wind energy that can be applied to the soil surface u_{*s} by that proportion which exceeds u_{*ts} . Notably, u_{*ts} provides information on the critical amount of aerodynamic cover required to inhibit wind erosion. Consequently, it provides valuable information for management.

We assumed that the heterogeneity of the transport within the pixel was represented by the albedo of the pixel and the area of the transport was defined by the pixel. This enabled the transport in one dimension (Q_h ; $\text{g m}^{-1} \text{s}^{-1}$) to be converted to an areal quantity by dividing by a MODIS pixel side (500 m) to produce wind erosion (E ; $\text{g m}^{-2} \text{s}^{-1}$). We calculated the amount of SOC removed by wind erosion. Unlike the selective removal of fine, SOC- and nutrient-rich material by dust emission (Chappell et al., 2013; Webb et al., 2013), we assumed that wind erosion is not selective. We multiplied E by the number of seconds in one year ($\text{g m}^{-2} \text{y}^{-1}$) and then divided by 100 to convert the units ($\text{t ha}^{-1} \text{y}^{-1}$).

2.2. Model data

The Google Earth Engine (GEE) provides a global geospatial platform for intensive parallel processing of satellite remote sensing and other environmental data (Gorelick et al., 2017). It currently contains MODIS (MCD43A1, collection 6) data which provides estimates of land surface albedo at 500 m globally every day for 2000-present. The GEE also includes the output from numerical weather forecasting and land surface models. Of relevance is the Global Land Data Assimilation System (GLDAS; Rodell et al., 2004), which provides global wind speed and soil moisture at 25 km resolution every 3 h for two periods (1948–2010 and 2000-present). The GLDAS ingests satellite and ground-based observational data products. The GLDAS-2.1 simulation data (2000-present) is forced with National Oceanic and Atmospheric Administration (NOAA)/Global Data Assimilation System (GDAS) atmospheric analysis fields, the disaggregated Global Precipitation Climatology Project (GPCP) precipitation fields, and the Air Force Weather Agency's AGRicultural METeorological modelling system (AGRMET) radiation fields. Using land surface modelling and data assimilation techniques, it generates optimal fields of land surface states and fluxes (Rodell et al., 2004).

We used existing soil data in the GEE from the SoilGrids dataset (Hengl et al., 2017) to estimate u_{*ts} including soil texture (clay $< 2 \mu\text{m}$, silt $< 50 \mu\text{m}$ and sand $< 2000 \mu\text{m}$) as a mass fraction at a depth of 0 m and soil organic carbon (SOC) the mass fraction of carbon by weight in the $< 2 \text{ mm}$ soil material (Fig. 4). This extant global map of soil organic carbon (SOC) content shows that semi-arid environments particularly around the low latitudes have much smaller amounts of SOC than other regions. The deserts, displayed in white-yellow, have the smallest SOC stocks. These regions occur in southern USA and Mexico and across Chile and Argentina. The majority of north Africa has very little SOC near the surface. A mega-region of small SOC stock occurs across the Arabian Peninsula, through Iran, China and Mongolia and the majority

of continental Australia.

The albedo-based wind erosion scheme above (Chappell and Webb, 2016) was coded in to the GEE making use of the MODIS albedo, GLDAS wind speed and soil moisture and SoilGrids soil organic carbon content and soil texture data. These data enable wind erosion estimates to be made at finer spatial and temporal resolution and for time periods not previously achieved by other schemes. The soil surface shear stress (u_{s*}) was calculated daily 2001–2016. It is derived from MODIS albedo and influenced by the roughness of all scales (plant canopy, grass coverage, stone cover, soil aggregates, etc.) which protects the soil surface from wind erosion. We applied the daily MODIS normalised difference snow index (MOD10A1) to avoid including smooth ice-snow surfaces in the estimates of wind erosion. We also used daily surface soil temperature from the GLDAS to remove situations in which bare but frozen soil would otherwise contribute to wind erosion. The wind erosion (E ; $t\ ha^{-1}\ y^{-1}$) was calculated for each pixel every day between 2001–2016 and the per-pixel mean was calculated and displayed as a map. To establish the SOC erosion by wind, we multiplied Q_h by the static SOC content ($g\ kg^{-1}$), assumed no enrichment of SOC in the eroded material relative to the surface soil, and repeated the procedure as for E .

2.3. Calibration data

The aeolian sediment transport model is based on albedo and when calibrated with wind tunnel data provides area-weighted estimates of the driving variable u_{s*} . To calibrate the model, we required consistent areal estimates of transport from measurements taken at many locations (within a study site or pixel). Unfortunately, there are very few area-weighted estimates of sediment transport because of their time-consuming acquisition and a tradition of taking few (often only one) sediment transport samples within a study area. The recently established US National Wind Erosion Research Network tackled this dearth of measurements (Webb et al., 2016). Many samples of sediment transport are collected approximately monthly from selected sites across US agroecological systems. Measurements of horizontal sediment flux (Q_h) were obtained using Modified Wilson and Cooke (MWAC) samplers at the Jornada Experimental Range (JER) in New Mexico, USA between June 2015 and December 2017 (Fig. 3a). These Q_h measurements were made approximately every month at four heights to 1 m above the soil surface at 27 locations across the measurement area (100 m x 100 m; 1 ha) using stratified random sampling (Fig. 3b). This experimental configuration provides an areal (area-weighted) average of the sediment flux which is currently unique in aeolian research monitoring (Webb et al., 2016). The areal Q_h accounts for the spatial distribution in the temporally varying factors which influence wind erosion across the measurement area including variation in vegetation height, spacing and density, soil erodibility, surface shear stress and soil moisture. These measurements of areal Q_h are essential for comparison with the albedo-

based estimates of Q_h made over 500 m pixels.

The coordinates of the centre of the JER network site were included in the GEE code. That location was used to identify the 500 m MODIS pixel and to extract for the measurement period the MODIS-based aerodynamic properties. Wind speed (U_h ; $m\ s^{-1}$) measurements made at 10 m above ground level at the JER network site were used outside the GEE to make estimates of Q_h using Eq. 1. The predicted Q_h was inverted against the measured Q_h to obtain the optimised value of the parameter c . The value of the parameter that minimised the square root of the mean square error (RMSE) or difference between measured and predicted Q_h , was accepted as optimised.

3. Results

3.1. Sediment transport calibration

Sediment transport was predicted at the JER field site where measurements were made at daily time-steps and then aggregated to approximately monthly intervals which coincided with the measurement intervals. The optimisation of the transport model (Eq. 5) against field measurements produced a $RMSE = 274\ g\ m^{-1}\ month^{-1}$ and showed that the model needs to be adjusted by $c = 4.59$ to match the magnitude of measured sediment transport. Fig. 5 shows the time series of measured Q_h at the JER field site and the model estimates using the optimised parameter values. Small magnitude events are represented by the model, but extremes (at this scale) are less well represented. It is not clear at this stage whether these extreme amounts of sediment transport originate from the pixel (autochthonous) or are external to the pixel (allochthonous). In any case, the performance of the model is adequate; the model predicts at approximately 95% confidence detectable difference in aeolian sediment transport at $274\ g\ m^{-1}\ month^{-1}$.

3.2. Global wind erosion and soil organic carbon (SOC) loss

Fig. 6a shows the surface shear stress scaled by freestream wind speed (u_{s*}/U_f) as a proportion of the maximum ($u_{s*}/U_f = 0.04$) which indicates the fraction of erodible soil exposed to wind (FEW; i.e., unsheltered). The mean value for the time period (2001–2016) is different in different regions and under different land use and land cover. The hyper-arid deserts of North Africa and Middle East have the least sheltering (smoothest surfaces). The next least sheltered soil surfaces occur across North and South America, the Sahelian region of Africa, deserts through Iran, Afghanistan, the Thar Desert in India and through China and Mongolia and Australia. The most sheltered surfaces and those least likely to contribute wind erosion are those with < 0.5 sheltering. They occur in the main cultivated regions and forested regions. Where the smoothest, least sheltered surfaces coincide with wind speeds which exceed the critical threshold (u_{*ts}), wind erosion will occur. Where seasonal variation changes the aerodynamic roughness

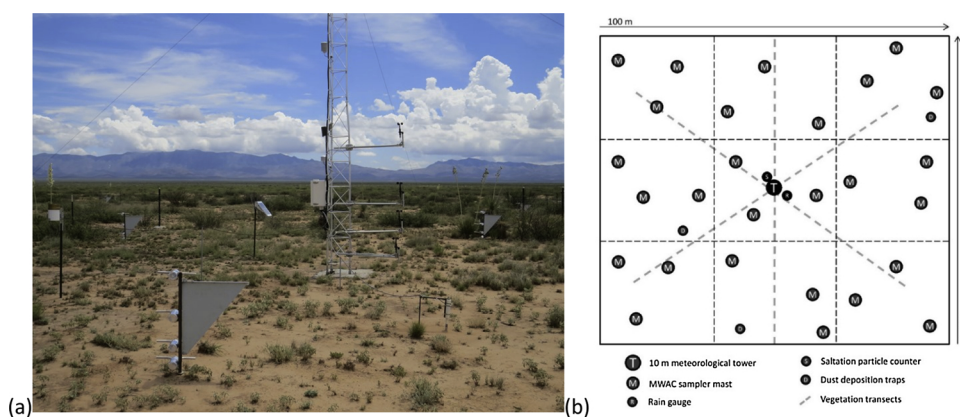


Fig. 3. The instrumented site at the Jornada Experimental Range (JER), New Mexico (a) and a schematic representation of the site showing the locations of the Modified Wilson and Cooke (MWAC) sediment samplers and other instruments (b).

Taken from the USA National Wind Erosion Research Network (<http://winderosionnetwork.org/>).

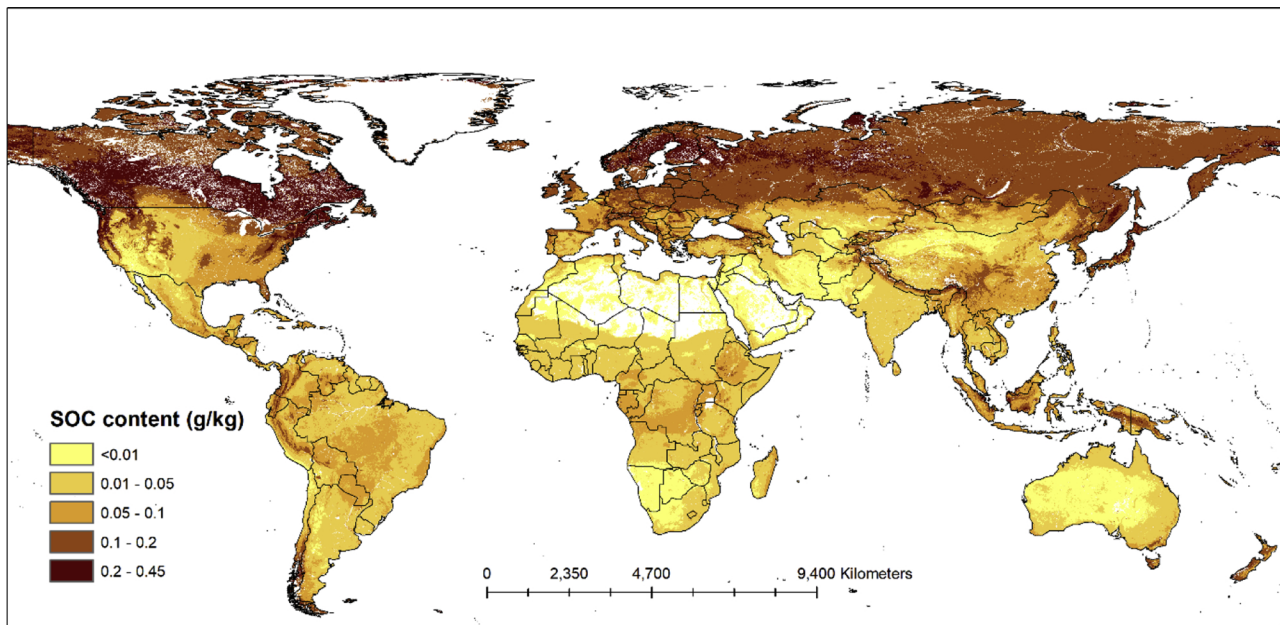


Fig. 4. Predicted soil organic carbon (SOC) content (g kg^{-1}) from the SoilGrids dataset (Hengl et al., 2017).

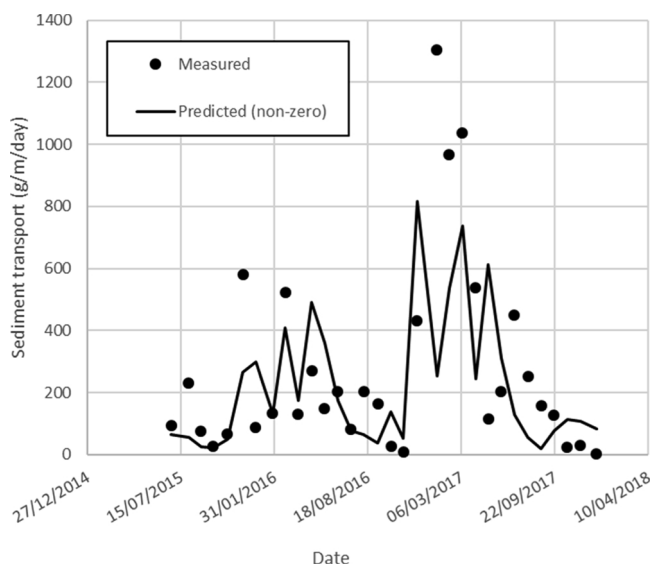


Fig. 5. Time series of horizontal sediment flux (Q_h) measured (black dots) approximately every month between June 2015 and December 2017. Predictions of Q_h were made every 3 h for the same period and then aggregated to match the measurement intervals (black line). The predictions were inverted against the measurements to optimise the values of the c model parameter.

e.g., in cultivated regions (across southern Europe, USA and Australia) or land use change or grazing has changed the vegetation cover (e.g., Amazon rain forest) the soil surface is exposed to wind erosion.

We found most wind erosion (E ; $\text{t ha}^{-1} \text{y}^{-1}$) occurs in regions of North Africa, the border between Iran and Afghanistan and the Gobi Desert of China and Mongolia (Fig. 6b). A considerably larger area of intermediate E occurs in the mega-region of drylands through Iran and Afghanistan, the Arabian Peninsula and across northern Africa. Similar magnitude of E is found in the dryland regions of USA and Mexico, Australia and Argentina and Chile. The margins of these regions contain the smallest magnitude of wind erosion but also cover a large area. Since the SOC content of drylands is typically small, the loss of SOC via wind erosion is minimal across most of the vast dryland regions (Fig. 6c). However, within all dryland regions there are areas where

SOC erosion is much larger. Intermediate SOC erosion occurs in the USA and Mexico and throughout the wind eroded region of southern America and the Sahel. Intermediate values of SOC erosion are also found through Persia and northern China and Mongolia. The largest global SOC erosion by wind occurs in Argentina, Sahelian Africa, Somalia and mostly in Mongolia where large SOC content coincides with large wind erosion.

To provide additional insight to the temporal variation of SOC erosion by wind within the global drylands, we plotted SOC erosion as an accumulation over time for 5 km sites in selected global drylands (Fig. 7a). The site in New South Wales, Australia, is an order of magnitude smaller than other sites and is barely discernible in its decline. In increasing order of magnitude, the sites in Namibia, the Tibetan Plateau and Mongolia show a linear rate of declining SOC erosion. In New Mexico, USA the SOC erosion was declining until 2008 and then the rate increased to 2010 after which it accelerated. Sites in southern Argentina, south-west Niger and Mauritania show a radical change in SOC erosion after 2010. After 2014 the greatest rate of SOC erosion changed from Mongolia to Mauritania. The only site to show declining SOC erosion is in northern Afghanistan after 2004.

The cause of these abrupt changes in SOC erosion are due to change in soil surface shear stress by the balance between changing vegetation cover (represented by FEW) and / or changing wind speed (Fig. 7b). The very rapid changes in SOC erosion are very likely to be due to change in wind speed. For example, the rapid decrease in SOC erosion in northern Afghanistan is very likely due mainly to a decrease in wind speed. Similarly, the rapid increase in SOC erosion in south-west Niger and Mauritania is very likely due mainly to an increase in wind speed after 2010. However, the linear increase in u_{S^*} in southern Argentina and Mongolia is much more likely to be caused by decreasing land surface aerodynamic roughness. Similarly, the linear decrease in u_{S^*} on the Namibian coast is more likely to be increasing aerodynamic roughness due to increased vegetation.

4. Discussion

4.1. Global wind erosion and SOC loss

The physically-based wind erosion model enables the identification of global locations where change in surface shear stress (u_{S^*}) occurs due

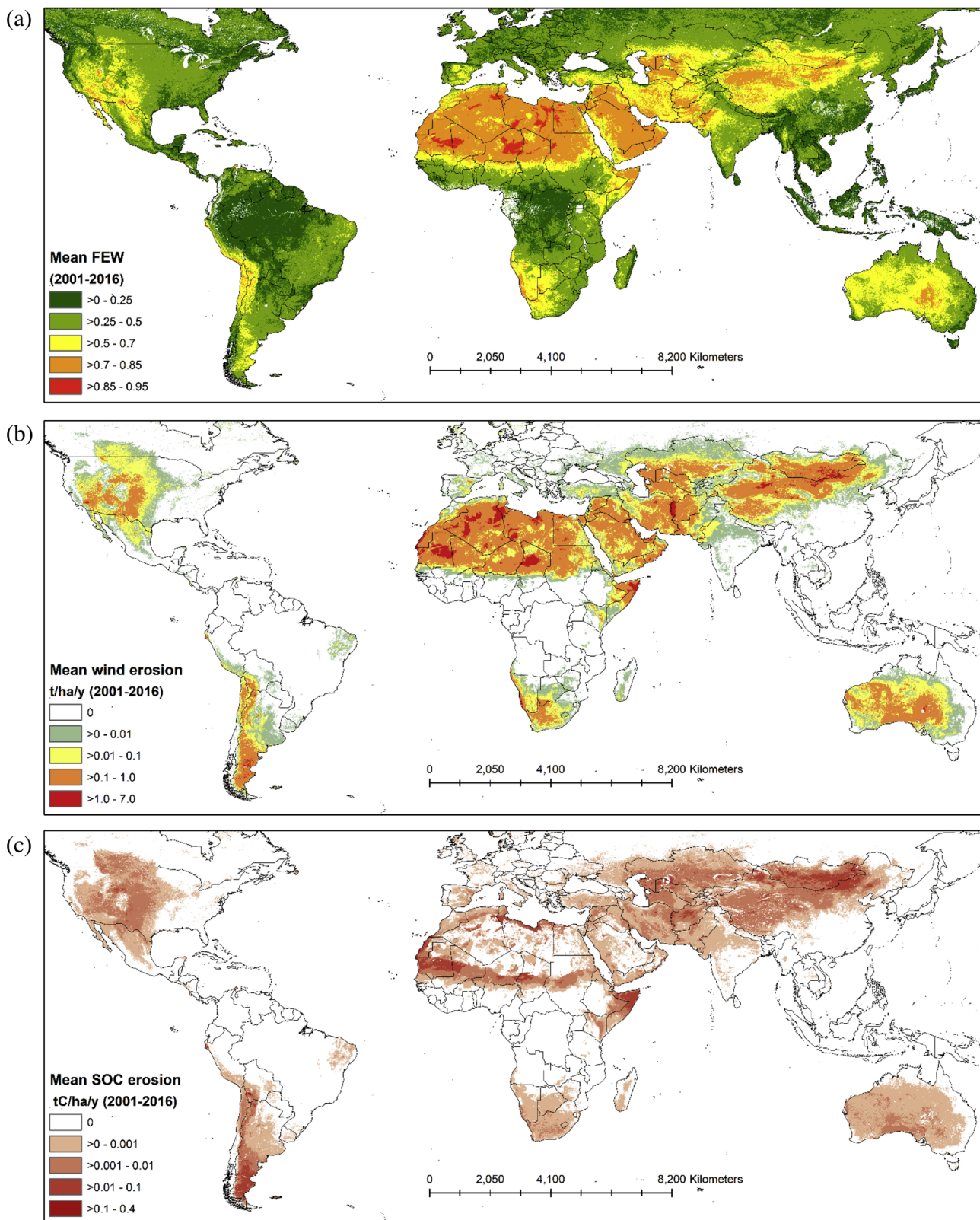


Fig. 6. Daily MODIS albedo (500 m; MCD43A1 collection 6), GLDAS (v2.1; 25 km) wind speed and soil moisture and SOC content and soil texture (250 m) data from the SoilGrids dataset (Hengl et al., 2017) used to produce over time (2001–2016) (a) surface shear stress u_{s*} scaled by freestream wind speed (u_{s*}/U_f ; dimensionless) as a proportion of the maximum ($u_{s*}/U_f = 0.04$) which indicates the fraction of erodible soil exposed to wind (FEW; i.e., unsheltered); (b) mean annual wind erosion (E ; $\text{t ha}^{-1} \text{y}^{-1}$) and (c) soil organic carbon erosion ($\text{tC ha}^{-1} \text{y}^{-1}$) by wind.

to seasonality and land use / land cover changes (Fig. 6a). The spatial patterns of u_{s*} for Australia are consistent with those identified nationally by Webb et al. (2006) and across the northern Lake Eyre Basin

by Webb et al. (2009) using an empirical land erodibility model. Typically, the largest change in u_{s*} occurs in cultivated regions and exposes the soil to wind erosion. Many of the locations where the largest

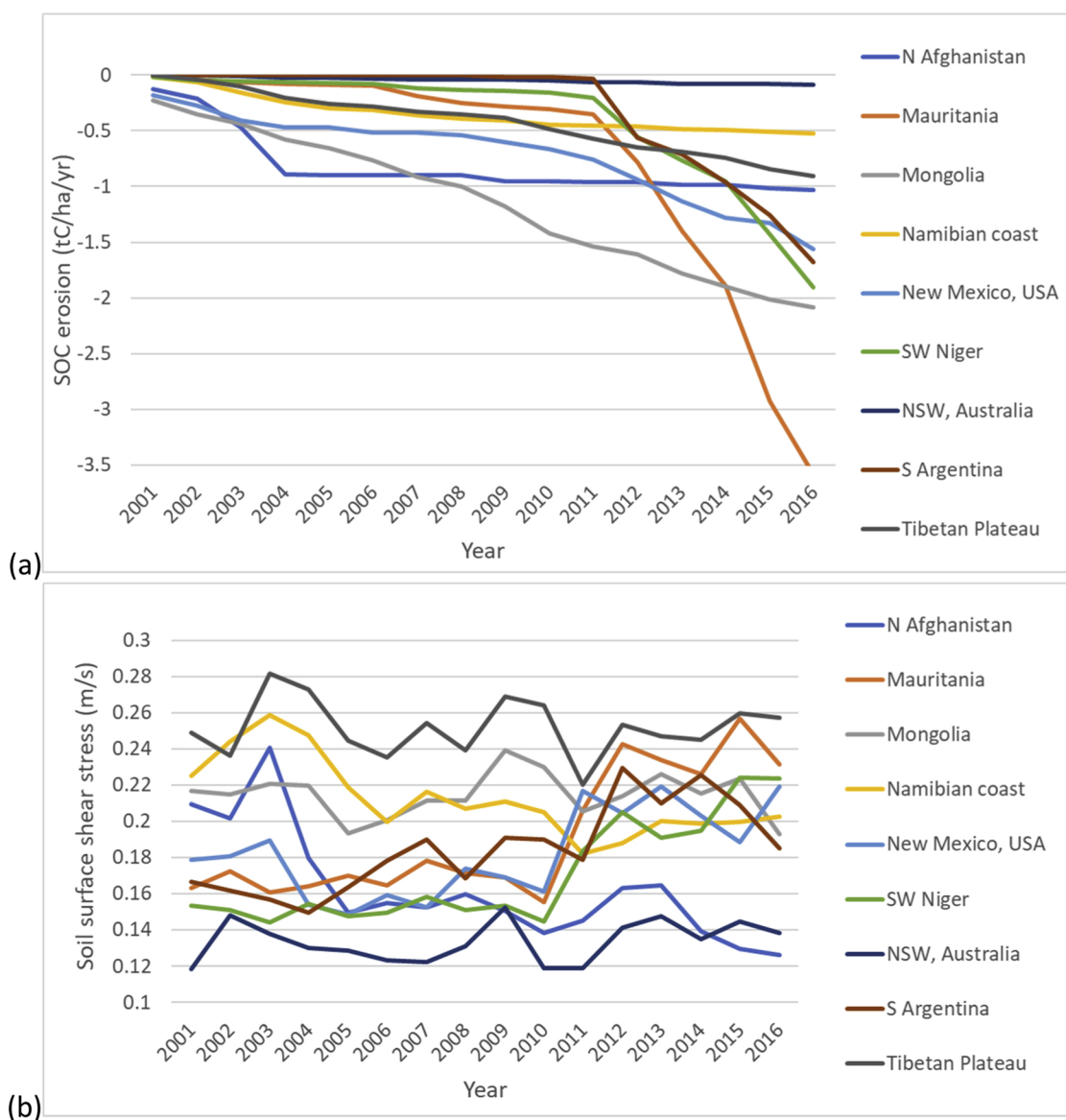


Fig. 7. Selected 5 km sites in global drylands during 2001–2016 showing accumulated soil organic carbon (SOC) erosion ($\text{tC ha}^{-1} \text{y}^{-1}$) removed by wind (a) and change in soil surface shear stress (u_{S^*} ; m s^{-1} ; b).

range in u_{S^*} occurs coincide with small wind erosion (Fig. 6b). However, rangelands cover a much larger area and have an intermediate range of u_{S^*} and the largest wind erosion. Most sediment transport (not dust emission) occurs across North Africa, the Middle East through Iran, Afghanistan and deserts in the China and Mongolia. The majority of extreme wind erosion occur in North Africa with notable exceptions on the border between Afghanistan and Iran and the Gobi desert crossing China and Mongolia.

The global cultivated regions have generally small wind erosion but large SOC content and consequently small to intermediate SOC erosion (Fig. 6c). The global rangelands have generally intermediate to large wind erosion but small SOC content and consequently intermediate to large SOC erosion. These findings are consistent with those of SOC dust emission for Australia (Chappell et al., 2013). The largest amount of SOC erosion by wind occurs across East Asia and particularly in northeastern China and Mongolia. Other global ‘hot’ spots of SOC erosion by wind are Mauritania, Somalia and southern Argentina. Notably, southern USA and Mexico have intermediate wind erosion but large SOC content and consequently SOC erosion in this region is perhaps the second largest global source. The SOC erosion is similar to that of

central Asia and the large global area of intermediate SOC erosion by wind which extends across northern China and Mongolia, the Sahel and north African coast, and southern Argentina.

The rate of SOC erosion by wind is evident from selected sites in these global drylands (Fig. 7). These sites show different rates of SOC removal and some which are accelerating and others which are decelerating. One aspect they have in common is that the SOC erosion is generally rapid. Few field measurements of SOC losses due to wind erosion are available for comparison, although Li et al. (2007) found similarly large rates of SOC erosion due to wind following grass removal in the Chihuahuan desert of southern New Mexico, USA. In our 16-year simulation period, the majority of sites have lost $> 1 \text{ tC ha}^{-1} \text{y}^{-1}$ by wind erosion and for the same time period in Mongolia the SOC eroded by wind is more than tripled ($> 3 \text{ tC ha}^{-1} \text{y}^{-1}$). Whilst the SOC content in the surface soil (0–10 cm) may be larger under crops and pastures compared with rangelands, SOC content may be surprisingly large at depth ($> 10 \text{ cm}$), particularly in some drylands. The location of SOC deep ($> 10 \text{ cm}$) in the soil profile may slow decomposition due to limited moisture and nutrients. In these situations, wind erosion and intermediate SOC content will persistently produce large SOC erosion

irrespective of the SOC returned to the soil via biomass/NPP (which is comparatively low). Consequently, in these situations SOC erosion will be dependent on the frequency of wind erosion rather than changing stock (with depth, time, productivity) of SOC. It is also possible that SOC erosion rates will decline with time following land cover change as SOC stocks and surface soil textures change.

SOC losses from dryland ecosystems and more mesic croplands are likely to have different impacts on the systems depending on the size of SOC stocks, proportional losses of SOC due to erosion, and SOC decomposition and replacement rates (Jackson et al., 2017). Wind erosion of SOC from dryland ecosystems, which have small SOC stocks, may have greater impact on ecosystem function (e.g., soil health and hydrology) and resilience to land management and abiotic drivers of land degradation than in croplands with larger SOC stocks (Lal, 2002). Dryland cropping systems, for example in the Sahel of West Africa, have been found to be particularly susceptible to the impacts of SOC erosion by wind where SOC stocks can be depleted in less than a decade. In Australia, it has been estimated that ignoring SOC erosion increases uncertainty in estimates of C stocks by between 0.08 to 0.27 tC ha⁻¹ yr⁻¹ (Sanderman and Chappell, 2013). This is within the expected SOC sequestration range of some options for agricultural management (0.11 to 0.75 tC ha⁻¹ yr⁻¹; (Conyers et al., 2015)). In these situations, avoided loss of SOC by reducing wind erosion may have more immediate benefits for decreasing land degradation compared with strategies focused on sequestration of SOC.

4.2. Global wind erosion model performance

There are no global studies of wind erosion for comparison with our results. However, there are a few regional assessments of wind erosion and many small (field) scale studies using ¹³⁷Cs to estimate medium-term (ca. 30–40 year average) estimates of soil erosion (Chappell et al., 2014). The challenge with using these studies is that in many dryland regions water erosion may combine with wind erosion to contribute to the measured change in ¹³⁷Cs. Van Pelt et al. (2016) used ¹³⁷Cs measurements to partition water erosion and deduce wind erosion of 3.7–6.6 t ha⁻¹ y⁻¹ at an experimental site near Bushland, Texas. At this location our model estimates wind erosion over the 16-year period to be up to 0.1 t ha⁻¹ y⁻¹. Ritchie et al. (2003) studied the patterns of soil redistribution in several plant communities in southern New Mexico using ¹³⁷Cs. They found interdune blowout areas representing erosion rates of 3.2 to 4.1 t ha⁻¹ yr⁻¹. Our model estimates of wind erosion were almost the same for that region (1.1 t ha⁻¹ y⁻¹). Our results for North America closely match the spatial patterns of dust-producing regions identified by Prospero et al. (2002) and Ginoux et al. (2012). Our model includes the Saskatoon region of Canada affected by wind erosion (e.g., Sutherland, 1994).

A recent empirical wind erosion modelling study for Europe shows a very similar pattern to our wind erosion results (Borrelli et al., 2016). Borrelli et al. (2016) did not quantify the erosion but the relative magnitude of wind erosion across the wind eroded region of Europe was similar to our results. Notably, our results for wind erosion in the East Anglian region of UK (0.2 t ha⁻¹ y⁻¹) were the same order of magnitude as the ¹³⁷Cs-derived estimates of wind erosion (0.6 t ha⁻¹ y⁻¹; Chappell and Warren, 2003).

In western China the Qinghai-Tibetan Plateau is a high altitude arid area that is prone to wind erosion. Yan et al. (2001) sampled multiple landforms and land use areas in the north-central and southern part of the region. They determined soil loss rates of 84.1, 69.4, 30.7, and 21.8 t ha⁻¹ yr⁻¹ for shrub-stabilized coppice dunes, semi-stabilized dunes, dryland farm fields, and grasslands, respectively, and for the entire Qinghai-Tibet Plateau, they estimated an annual soil loss rate of 47.6 t ha⁻¹ y⁻¹ (Van Pelt, 2013). These rates are an order of magnitude larger than our findings of 1.6 t ha⁻¹ y⁻¹. In Inner Mongolia, increased grazing pressure increased the susceptibility of the region to wind erosion. Funk et al. (2012) used ¹³⁷Cs to estimate wind erosion at 0.5–

1.7 t ha⁻¹ y⁻¹ in the valley and windward slope. At the same location our results, albeit for a 16-year period showed wind erosion to be up to 1.3 t ha⁻¹ y⁻¹.

On a transect of Western Australia, Chappell and Baldock (2016) used ¹³⁷Cs measurements across six 50 ha fields and estimated wind erosion at 4.4 ± 2.1 t ha⁻¹ y⁻¹. Our model results for the same locations and part of the same period for wind erosion were up to 0.3 t ha⁻¹ y⁻¹ and for SOC erosion up to 0.003 t C ha⁻¹ y⁻¹. The measured rate had increased relative to an earlier modelled phase suggesting that conservation agriculture had not reduced wind erosion in this region. This study is one of very few which also measured the loss of SOC, reporting up to 0.2 t C ha⁻¹ y⁻¹ had been lost from these fields. Of particular relevance here is that SOC erosion was similar to measured sequestration rates in the region (up to 0.5 t C ha⁻¹ y⁻¹; 10 years) for many management practices recommended for building SOC stocks. Chappell and Baldock (2016) showed that if SOC erosion is equal to (or greater than) the increase in SOC due to management practices, the change will not be detectable (or a loss will be evident). Furthermore, Chappell and Baldock (2016) suggested that “...without including soil erosion in SOC sequestration calculations, the monitoring of SOC stocks will lead to, at best the inability to detect change and, at worst the false impression that management practices have failed to store SOC”.

4.3. Implications for Land Degradation Neutrality indicators

Land Degradation-Neutrality (LDN) aims to maintain and / or renew the global resource of healthy and productive land by avoiding, reducing, or reversing degradation. By understanding where wind erosion is occurring globally, rather than just where cover is small, land management intervention programs can be prioritised. Because u_{S^*} describes the surface roughness, places with stone cover or other non-biotic cover are accounted for in their extent of protection / sheltering from the wind. By linking wind erosion to SOC, this study shows that SOC stocks are dynamic and threatened by wind erosion in arid drylands. In such areas, the resilience of the soil is under threat and continued wind erosion will compromise their productive potential, ultimately leading to more degraded and retired agricultural land and greater pressure on other areas for production. Consequently, it is feasible to link u_{S^*} or more specifically FEW to an economic assessment e.g., taking in to account how SOC is priced for C sequestration or the cost of using fertiliser to replace soil nutrients removed by wind erosion. Land management decisions that increase FEW, e.g., by increasing grazing intensity and duration and otherwise manipulating land cover, can be directly linked to wind erosion and the economics associated with loss in SOC and soil nutrients. In extensive grazing systems typical of the rangelands, loss of SOC and nutrients can lead to irreversible land use and vegetation change due to the often uneconomic cost of replacing nutrients in these systems. Valuing SOC and nutrients through this approach would enable a full economic costing for the decision-making process.

Some land management practices have caused considerable degradation in some dryland regions. Consequently, it will likely take considerable time to manage degraded lands back to a productive and resilient condition. In other regions where the land is in a desirable condition, the FEW can be used to provide early warning of degradation e.g., during drought or other unforeseen circumstance or highlight those areas at greatest risk of SOC erosion and land degradation. Perhaps most importantly, land managers can set a locally relevant level of FEW for a tolerable amount of wind erosion and establish trigger points for management intervention. Although not shown here, similar global patterns of nitrogen and phosphorous losses are also expected to occur. The patterns are perturbed by small differences in the geographical distribution of nutrient stocks. With tools like the wind erosion model used here, erosion effects on nutrient and SOC stocks could be considered simultaneously in assessments of LDN.

5. Conclusion

The work presented here provides clear, unambiguous evidence that one of the key indicators for LDN, soil organic carbon (SOC) is declining due to wind erosion:

- 1) SOC does not change slowly from the net effects of biomass and disturbance / removal because SOC can be removed rapidly by wind erosion, particularly after land use and land management induced cover change;
- 2) in the presence of wind erosion, SOC cannot be an indicator of resilience because it cannot recover quickly; the SOC erosion is similar to SOC productivity particularly in drylands;
- 3) SOC erosion by wind occurs to a large magnitude in every global region of the vast Earth's drylands (45% of the land surface). The substantial amount of SOC change is negative;
- 4) on these bases, omission of SOC erosion from the LDN framework as a key process would likely cause inaccurate assessments of resource condition and highly uncertain policy advice.

We appreciate that the LDN indicator of land cover provides a metric of land use effects on ecosystems e.g., land conversion. Unless these metrics are applied at an appropriate frequency, they will not provide a dynamic response. In contrast, we have shown that by replacing land cover with u_s^* specific for wind erosion, and then focusing on erosion, we are able to quantify the dynamic impact of a key land degradation process on the soil resource (specifically SOC). Most fundamentally, we have shown that loss of SOC, particularly in drylands, is most likely to be due to wind erosion. Since LDN is focused on maintaining healthy and productive land, and SOC levels are linked to soil health, we believe this approach improves the chances of monitoring and achieving LDN. We recommend that land cover is supplemented with estimates of wind erosion for the global dryland regions of the world due to its dynamic impact on SOC.

Acknowledgements

We are grateful for the resources provided by the Google Earth Engine (GEE) and the technical support of its forum and in particular the help from Noel Gorelick in getting this work coded. We appreciate the GLDAS, MODIS and SoilGrids data made available via the GEE. Thanks to Stephan Heidenreich for help with the figures and two anonymous reviewers for their comments. John Leys was supported by the Environmental Accounting and Reporting projected funded by the Science Division, Office of Environment and Heritage

References

Amundson, R., Berhe, A.A., Hopmans, J.W., Olson, C., Sztein, A.E., Sparks, D.L., 2015. Soil and human security in the 21st century. *Science* 348 (May), 6235. <https://doi.org/10.1126/science.1261071>.

Bestelmeyer, B.T., Okin, G.S., Duniway, M.C., et al., 2015. Desertification, land use, and the transformation of global drylands. *Front. Ecol. Environ.* 13, 28–36.

Borrelli, P., Panagos, P., Ballabio, C., Lugato, E., Weynants, M., Montanarella, L., 2016. Towards a pan-european assessment of land susceptibility to wind erosion. *Land Degrad. Develop.* 27, 1093–1105.

Chappell, A., Baldock, J., 2016. Wind erosion reduces soil organic carbon sequestration falsely indicating ineffective management practices. *Aeolian Res.* 22, 107–116. <https://doi.org/10.1016/j.aeolia.2016.07.005>.

Chappell, A., Warren, A., 2003. Spatial scales of ^{137}Cs -derived soil flux by wind in a 25 km² arable area of eastern England. *Catena* 52, 209–234. [https://doi.org/10.1016/S0341-8162\(03\)00015-8](https://doi.org/10.1016/S0341-8162(03)00015-8).

Chappell, A., Webb, N., 2016. Using albedo to reform wind erosion modelling, mapping and monitoring. *Aeolian Res.* 23, 63–78.

Chappell, A., Dong, Z., Van Pelt, S., Zobeck, T., 2010. Estimating aerodynamic resistance of rough surfaces using angular reflectance. *Remote Sens. Environ.* 114 (7), 1462–1470.

Chappell, A., Webb, N.P., Butler, H., Strong, C., McTainsh, G.H., Leys, J.F., Viscarra Rossel, R., 2013. Soil organic carbon dust emission: an omitted global source of atmospheric CO₂. *Glob. Change Biol.* 19, 3238–3244.

Chappell, A., Webb, N.P., Viscarra Rossel, R.A., Bui, E., 2014. Australian net (1950s–1990) soil organic carbon erosion: implications for CO₂ emission and land-atmosphere modelling. *Biogeosciences* 11, 5235–5244.

Chappell, A., Baldock, J., Sanderman, J., 2015. The global significance of omitting soil erosion from soil organic carbon cycling models. *Nat. Clim. Change* 2015 (December). <https://doi.org/10.1038/nclimate2829>.

Chappell, A., Webb, N.P., Guerschman, J.P., Thomas, D.T., Mata, G., Hancock, R., Leys, J.F., Butler, H., 2017. Improving ground cover monitoring for wind erosion assessment using lateral cover derived from MODIS BRDF parameters. *Remote Sens. Environ.* <https://doi.org/10.1016/j.rse.2017.09.026>.

Conyers, M., Liu, D.L., Kirkegaard, J., Orgill, S., Oates, A., Li, G., Poile, G., Kirkby, C., 2015. A review of organic carbon accumulation in soils within the agricultural context of southern New South Wales, Australia. *Field Crops Res.* 184, 177–182.

Cowie, A.L., Orr, B.J., Castillo Sanchez, V.M., Chasek, P., Crossman, N.D., Erlewein, A., Louwagie, G., Maron, M., Metternicht, G.I., Minelli, S., Tengberg, A.E., Walter, S., Welton, S., 2018. Land in balance: the scientific conceptual framework for Land Degradation Neutrality. *Environ. Sci. Policy* 79, 25–35.

Dialynas, Y.G., Bastola, S., Bras, R.L., Billings, S.A., Markewitz, D., Dd, Richter, 2016. Topographic variability and the influence of soil erosion on the carbon cycle. *Global Biogeochem. Cycles* 30 (5), 644–660.

Doetterl, S., Van Oost, K., Six, J., 2012. Towards constraining the magnitude of global agricultural sediment and soil organic carbon fluxes. *Earth Surf. Process. Landforms* 37, 642–655.

Ellerbrock, R.H., Gerke, H.H., Deumlich, D., 2016. Soil organic matter composition along a slope in an erosion-affected arable landscape in North East Germany. *Soil Tillage Res.* 156, 209–218.

Elliott, E.T., 1986. Aggregate structure and carbon, nitrogen, and phosphorus in native and cultivated soils. *Soil Sci. Soc. Am. J.* 50 (3), 627–633.

Faeth, P., Crosson, P., 1994. Building the case for sustainable agriculture. *Environment* 36 (1), 16–20.

FAO, ITPS, 2015. The Status of the World's Soil Resources (Main Report). Food and Agriculture Organization of the United Nations, Rome 2015.

Fecan, F., Marticorena, B., Bergametti, G., 1999. Parameterization of the increase of the aeolian erosion threshold wind friction velocity due to soil moisture for arid and semi-arid areas. *Ann. Geophys. Discuss.* 17, 149–157. <https://doi.org/10.1007/s005850050744>.

Funk, R., Li, Y., Hoffmann, C., Reiche, M., Zhang, Z., Li, J., Sommer, M., 2012. Using ^{137}Cs to estimate wind erosion and dust deposition on grassland in Inner Mongolia-selection of a reference site and description of the temporal variability. *Plant Soil* 351 (2012), 293–307. <https://doi.org/10.1007/s11104-011-0964-y>.

Ginoux, P., Prospero, J.M., Gill, T.E., Hsu, N.C., Zhao, M., 2012. Global-scale Attribution of Anthropogenic and Natural Dust Sources and Their Emission Rates Based on MODIS Deep Blue Aerosol Products. *Reviews of Geophysics*. 50, RG3005.

Gorelick, N., Hancher, M., Dixon, M., Ilyushchenko, S., Thau, D., Moore, R., 2017. Google earth engine: planetary-scale geospatial analysis for everyone. *Remote Sens. Environ.* (in press).

Gregorich, E.G., Greer, K.J., Anderson, D.W., Liang, B.C., 1998. Carbon distribution and losses: erosion and deposition effects. *Soil Tillage Res.* 47 (3–4), 291–302.

Hengl, T., Mendes de Jesus, J., Heuvelink, G.B.M., Ruiperez Gonzalez, M., Kilibarda, M., et al., 2017. SoilGrids250m: global gridded soil information based on Machine Learning. *PLoS One* 12 (2), e0169748. <https://doi.org/10.1371/journal.pone.0169748>.

Jackson, R.B., Lajtha, K., Crow, S.E., Hugelius, G., Kramer, M.G., Piñeiro, G., 2017. The ecology of soil carbon: pools, vulnerabilities, and biotic and abiotic controls. *Annu. Rev. Ecol. Evol. Syst.* 48, 419–445.

Lal, R., 1990. Soil erosion and land degradation. In: Lal, R., Stewart, B.A. (Eds.), *The Global Risks*. Springer-Verlag, New York, pp. 129–172. Soil degradation.

Lal, R., 1995. Erosion-crop productivity relationships for soils of Africa. *Soil Sci. Soc. Am. J.* 59, 661–667.

Lal, R., 2002. Soil carbon dynamics in cropland and rangeland. *Environ. Pollut.* 116, 353–362.

Lal, R., 2003. Soil erosion and the global carbon budget. *Environ. Int.* 29 (4), 437–450.

Lal, R., 2004. Soil carbon sequestration impacts on global climate change and food security. *Science* 304 (5677), 1623–1627.

Lal, R., 2005. Soil erosion and carbon dynamics. *Soil Tillage Res.* 81 (2), 137–142.

Leys, J.F., Heidenreich, S.K., Strong, C.L., McTainsh, G.H., Quigley, S., 2011. PM10 concentrations and mass transport during “Red Dawn” - Sydney 23 September 2009. *Aeolian Res.* 3, 327–342.

Li, J., Okin, G.S., Alvarez, L., Epstein, H., 2007. Quantitative effects of vegetation cover on wind erosion and soil nutrient loss in a desert grassland of southern New Mexico, USA. *Biogeochemistry* 85, 317–332.

Li, Y., Yu, H., Chappell, A., Zhou, N., Funk, R., 2014. How much soil organic carbon sequestration is due to conservation agriculture reducing soil erosion? *Soil Res.* 52 (7), 717–726.

Luyssaert, S., et al., 2014. Land management and land cover change have impacts of similar magnitude on surface temperature. *Nat. Clim. Change*. <https://doi.org/10.1038/NCLIMATE2196>.

Nguyen, B., Lehmann, J., Kinyangi, J., Smernik, R., Riha, S., Engelhard, M., 2008. Long-term black carbon dynamics in cultivated soil. *Biogeochemistry* 89 (3), 295–308.

Parton, W.J., Schimel, D.S., Cole, C.V., Ojima, D.S., 1987. Analysis of factors controlling soil organic matter levels in Great Plains grasslands. *Soil Sci. Soc. Am. J.* 51, 1173–1179.

Pimentel, D., 1993. *World Soil Erosion and Conservation*. Cambridge University Press, Cambridge, UK.

Prospero, J.M., Ginoux, P., Torres, O., Nicholson, S.E., Gill, T.E., 2002. Environmental characterization of global sources of atmospheric soil dust identified with the Nimbus 7 Total Ozone Mapping Spectrometer (TOMS) absorbing aerosol product. *Rev. Geophys.* 40, 1. <https://doi.org/10.1029/2000RG000095>.

Raupach, M.R., 1992. Drag and drag partition on rough surfaces. *Boundary-Layer*

- Meteorol. 60, 374–396.
- Regnier, P., Fridlingstein, P., Giais, P., Mackenzie, F.T., Gruber, N., Janssens, I.A., Laruelle, G.G., Lauerwald, R., Luysaert, S., Andersson, A.J., 2013. Anthropogenic perturbation of the carbon fluxes from land to ocean. *Nat. Geosci.* 6, 597–607. <https://doi.org/10.1038/ngeo1830>.
- Ritchie, J.C., Herrick, J.E., Ritchie, C.A., 2003. Variability in soil redistribution in the northern Chihuahuan Desert based on 1371489 Cesium measurements. *J. Arid Environ.* 55, 737–746.
- Rodell, M., Houser, P.R., Jambor, U., Gottschalk, J., Mitchell, K., Meng, C.-J., Arsenault, K., Cosgrove, B., Radakovich, J., Bosilovich, M., Entin, J.K., Walker, J.P., Lohmann, D., Toll, D., 2004. The global land data assimilation system. *Bull. Amer. Meteor. Soc.* 85 (3), 381–394.
- Sanderman, J., Chappell, A., 2013. Uncertainty in soil carbon accounting due to unrecognized soil erosion. *Glob. Change Biol.* 19 (1), 264–272.
- Shao, Y., Raupach, M.R., Leys, J.F., 1996. A model for predicting aeolian sand drift and dust entrainment on scales from paddock to region. *Aust. J. Soil Res.* 34, 309–342.
- Singh, S., Singh, J.S., 1996. Water-stable aggregates and associated organic matter in forest, savanna, and cropland soils of a seasonally dry tropical region, India. *Biol. Fertil. Soils* 22 (1–2), 76–82.
- Sommer, M., Augustin, J., Kleber, M., 2016. Feedbacks of soil erosion on SOC patterns and carbon dynamics in agricultural landscapes—the CarboZALF experiment. *Soil Tillage Res.* 156, 182–184.
- Stallard, R.F., 1998. Terrestrial sedimentation and the carbon cycle: coupling weathering and erosion to carbon burial. *Global Biogeochem. Cycles* 12 (2), 231–257.
- Sutherland, R.A., 1994. Spatial variability of 137Cs and the influence of sampling on estimates of sediment redistribution. *Catena* 21, 57–71.
- Todd-Brown, K.E.O., Randerson, J.T., Post, W.M., Hoffman, F.M., Tarnocai, C., Schuur, E.A.G., Allison, S.D., 2013. Causes of variation in soil carbon simulations from CMIP5 Earth system models and comparison with observations. *Biogeosciences* 10 (3), 1717–1736.
- UNCCD, 2015. Bonn: United Nations Convention to Combat Desertification Report of the Conference of the Parties on its Twelfth Session, held in Ankara from 12 to 23 October 2015. Part Two: Actions Taken by the Conference of the Parties at Its Twelfth Session. ICCD/COP(12)/20/Add2015. Report of the Conference of the Parties on its Twelfth Session, held in Ankara from 12 to 23 October 2015. Part Two: Actions Taken by the Conference of the Parties at Its Twelfth Session. ICCD/COP(12)/20/Add. UN-Habitat-GLTN, 2016. Scoping and Status Study on Land and Conflict: Towards UN System-Wide Engagement at Scale. United Nations Human Settlements Programme Report 5/2016.
- Van Oost, K., Quine, T.A., et al., 2007. The impact of agricultural soil erosion on the global carbon cycle. *Science* 318 (5850), 626–629.
- Van Pelt, R.S., 2013. Use of anthropogenic radioisotopes to estimate rates of soil redistribution by wind I: Historic use of 137Cs. *Aeolian Res.* 9, 89–102. <https://doi.org/10.1016/j.aeolia.2012.11.004>.
- Van Pelt, R.S., Hushmurodov, S.X., Baumhardt, R.L., Chappell, A., Nearing, M.A., Polyakov, V.O., Strack, J.E., 2016. The reduction of partitioned wind and water erosion by conservation agriculture. *Catena*. <https://doi.org/10.1016/j.catena.2016.07.004>.
- Webb, N.P., McGowan, H.A., Phinn, S.R., McTainsh, G.H., 2006. AUSLEM (AUStralian Land Erodibility Model): a tool for identifying wind erosion hazard in Australia. *Geomorphology* 78, 179–200.
- Webb, N.P., McGowan, H.A., Phinn, S.R., McTainsh, G.H., Leys, J.F., 2009. Simulation of the spatiotemporal aspects of land erodibility in the northeast Lake Eyre Basin, Australia, 1980–2006. *J. Geophys. Res.* 114, F01013. <https://doi.org/10.1029/2008JF001097>.
- Webb, N.P., Strong, C.L., Chappell, A., Marx, S.K., McTainsh, G.H., 2013. Soil organic carbon enrichment of dust emissions: magnitude, mechanisms and its implications for the carbon cycle. *Earth Surf. Process. Landf.* 38, 1662–1671.
- Webb, N.P., Herrick, J.E., Van Zee, J.W., et al., 2016. The National Wind Erosion research Network: building a standardized long-term data resource for aeolian research, modeling and land management. *Aeolian Res.* 22, 23–36.
- Webb, N.P., Marshall, N.A., Stringer, L.C., Reed, M.S., Chappell, A., Herrick, J.E., 2017. Land degradation and climate change: building climate resilience in agriculture. *Front. Ecol. Environ.* 15, 450–459.
- WHO, 2004. World Health Report. http://www.who.int/whr/2004/annex/topic/en/annex_2-en.pdf. (10/1/04) (NB. Other WHO reports for previous years can be accessed through this site).
- Yan, P., Dong, Z., Dong, G., Zhang, X., Zhang, Y., 2001. Preliminary results of using ¹³⁷Cs to study wind erosion in the Qinghai-Tibet Plateau. *J. Arid Environ.* 47, 443–452.